Thermoresponsive Copolymer Hydrogels Based on *N*-Isopropylacrylamide and Cationic Surfactant Monomers Prepared from Micellar Solution and Microemulsion in a One-Step Reaction

Tatjana Friedrich and Bernd Tieke*

Department Chemie, Universität zu Köln, Luxemburger Str. 116, D-50939 Köln, Germany

Mathias Meyer and Wim Pyckhout-Hintzen

Institut für Festkörperforschung, Neutronenstreuung, Forschungszentrum Jülich, Postfach 1913, D-52425 Jülich, Germany

Vitaly Pipich

Institut für Festkörperforschung, Forschungszentrum Jülich, Jülich Centre for Neutron Science at FRM II, Lichtenbergstr. 1, D-85747 Garching, Germany

Received: November 30, 2009; Revised Manuscript Received: March 16, 2010

Thermoresponsive hydrogels were prepared upon radiation-induced copolymerization of aqueous micellar solutions containing *N*-isopropylacrylamide (NiPAAm) and a cationic surfactant monomer (surfmer), and of microemulsions containing NiPAAm, surfmer, and styrene. Three surfmer compounds were used: (11-(acryloyloxy)undecyl)trimethylammonium bromide (AUTMAB), (11-(methacryloyloxy)undecyl)trimethylammonium bromide (MUTMAB), and (2-(methacryloyloxy)ethyl)dodecyldimethylammonium bromide (MEDDAB). Comonomer solutions were studied on their phase behavior and structure using small-angle neutron scattering (SANS). The presence of surfmers increased the solubility of NiPAAm in the aqueous phase. SANS studies indicate that the surfmers form spherical micelles, which in the presence of styrene are increased and in the presence of NiPAAm are decreased in size. Styrene is incorporated in the core, and NiPAAm is incorporated in the shell of the micelles. If styrene and NiPAAm are present, the effects of both compensate each other, the micelle size remains unchanged, and only small amounts of styrene are solubilized. Evaluation of scattering curves indicated remarkable changes in headgroup dissociation of surfmers in the presence of NiPAAm in the micellar solutions. If exposed to ^{60}Co-gamma irradiation (dose: 80 kGy), stable, transparent, and thermoresponsive hydrogels were directly obtained. The lower critical solution temperature (LCST) of gels containing surfmer in low concentration was higher than that for pure NiPAAm gels, whereas in gels with high surfmer concentration it was lower. The lowest LCST was observed if MEDDAB was present in the gel. 1 % (w/w) was already sufficient to lower the LCST from 33.2 to 28.5 °C. Gels with low surfmer concentration ($\leq$1 wt %) exhibited a strong, rapid swelling in water at 20 °C and a rapid and reversible shrinking at 50 °C. For a gel containing 1% AUTMAB, the swelling ratio was 2.4 times higher (MUTMAB, 2.8; MEDDAB, 1.5) than that for a pure NiPAAm gel. Copolymer gels containing more than 1 wt % surfmer exhibited a strong and rapid swelling below and above the LCST, because the copolymerized ionic surfmer induced an osmotic pressure in the gel. The effects of a variation of NiPAAm and surfmer concentration were studied, and the origins of the thermoresponsive properties are discussed.

1. Introduction

The preparation of so-called "intelligent" or "smart" hydrogels has attracted much attention in soft matter research in recent years.[1] "Intelligent" hydrogels are polymer networks with high water content able to undergo reversible phase transitions upon changes in temperature,[2] pH,[3] magnetic field,[4] light,[5] solvent,[6] and ionic strength.[7] *N*-Isopropylacrylamide (NiPAAm)-based hydrogels are known to change volume and transparency upon heating to temperatures above 32 °C, the lower critical solution temperature (LCST) of the gel.[8]

The possibility to tailor chemical and physical properties of hydrogels at the molecular level is an important prerequisite for technical applications in the fields of sensors, actuators, and drug delivery systems.[9] One way to decisively alter the properties is to incorporate and eventually copolymerize surfactants in NiPAAm-based hydrogels. Surfactant incorporation increases the amphiphilicity of the gel, which alters the LCST and the swelling/shrinking behavior. Up to now, only few attempts were made to prepare copolymer hydrogels based on NiPAAm and surfactant monomers (surfmers). Probably the earliest attempt was made by Yu and Grainger,[10] who prepared amphiphilic thermosensitive terpolymer hydrogels by micellar polymerization of NiPAAm, long chain *N*-alkylacrylamides, and sodium acrylate in aqueous medium. In this system, *N*-alkylacrylamides were stabilized by cosurfactants such as sodium dodecylsulfate. In subsequent studies, at first, the surfmer was polymerized followed by NiPAAm polymerization,[11,12] or

* Author to whom correspondence should be addressed. E-mail: tieke@uni-koeln.de. Phone: +492214702440. Fax: +494702217300.

10.1021/jp911358z
Published on Web 04/15/2010

SCHEME 1: Structure Model of the Polymerization in Aqueous Micellar NiPAAm−Surfmer Solution[a]

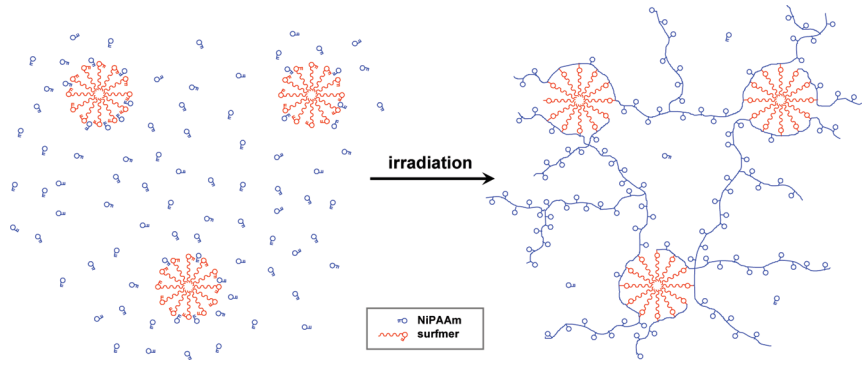

[a] A multiblock copolymer is obtained, in which poly-surfmer blocks (red) form micellar aggregates, while the poly-NiIPAAm blocks (blue) connect the individual micelles.

at first a linear NiPAAm−surfmer copolymer or macromonomer was prepared and subsequently cross-linked or copolymerized with additional NiPAAm to yield the hydrogel.[13] Most of the studies report on improved thermoresponsive behavior, such as ultrarapid shrinking[12] or rapid swelling and collapse.[11] Other properties such as structure and mechanical stability[14] or relations between structure and composition of the hydrogels and their thermoresponsive properties were only scarcely studied. There is very little information on the effect of the amount of surfmer and NiPAAm on the thermoresponsive properties, and the influences of a structural variation of the surfmers were not systematically studied as well. Mostly nonionic or anionic polymerizable amphiphiles were used as monomers, whereas cationic surfmers were not included or copolymerized in NiPAAm hydrogels. Formation of transparent hydrogels during a microemulsion polymerization was only scarcely studied,[15,16] and microemulsion polymerization of NiPAAm has not been reported yet.

Our work differs from previous work on surfactant-containing NiPAAm hydrogels in several points. First, NiPAAm and surfmer are copolymerized in micellar solution in a one-step reaction. Second, the reaction is brought about using 60-cobalt gamma irradiation. Third, for the first time, cationic surfmers are used for copolymerization with NiPAAm. The preparation route is outlined in Scheme 1. High energy irradiation is advantageous because polymerization can be carried out at room temperature and no additional compounds such as initiator, catalyst, and cross-linker are needed. It was hoped that the new preparation route might lead to hydrogels exhibiting several advantages compared with pure poly-NiPAAm hydrogels. First, the surfmers form micelles, which after polymerization represent physical cross-linking units being able to improve the mechanical stability of the gel. Second, the hydrophobic core (and the positively charged, hydrophilic shell) can be used to solubilize molecules (or counterions) able to modify the properties of the gel and to induce functionality in a simple manner.

In a recent communication, we already reported that thermoresponsive hydrogels can be prepared in a single-step route upon 60-cobalt gamma irradiation of a micellar aqueous solution of NiPAAm and 11-acryloylundecyltrimethylammonium bromide (AUTMAB) as surfmer.[17] The purpose of the present article is to present a comprehensive study of NiPAAm-based hydrogels containing either AUTMAB, 11-methacryloylundecyltrimethylammonium bromide (MUTMAB), or 2-methacryloylethyldodecyldimethylammonium bromide (MEDDAB) as surfmer. The molecular structures are shown in Scheme 2. The surfmers were chosen because they recently have been proven

SCHEME 2: Molecular Structures of MEDDAB, AUTMAB, and MUTMAB

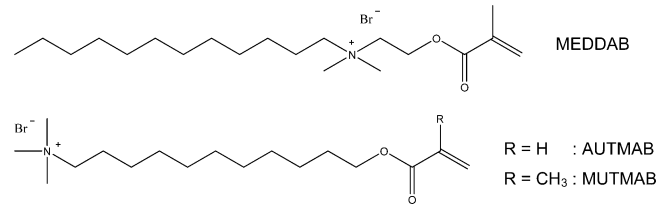

useful for copolymerization in microemulsion,[16] and homo- and copolymerization with acrylamide,[18,19] styrene,[20] or 2-hydroxyethyl methacrylate[21] in lyotropic mesophase. Structure studies using SANS and SAXS indicated that copolymerization always proceeded with retention of the macroscopic order of the system.

In the present study, phase diagrams of ternary NiPAAm−surfmer−water systems and quaternary systems containing additional styrene are presented, structural studies on the monomeric systems using small-angle neutron scattering are described, and the "intelligent" properties of the gels such as changes in volume and transparency upon temperature variation and variation of the NiPAAm and surfmer content of the system are reported and compared. A detailed study of the mechanical properties of the gels is the subject of a forthcoming publication,[22] as well as the introduction of functional properties via counterion exchange.[23] In this article, it is demonstrated that the three surfmers are suitable as comonomers for preparation of thermoresponsive surfmer−NiPAAm and styrene−surfmer−NiPAAm-copolymer networks.

2. Experimental Section

2.1. Materials. The cationic surfactant monomers were prepared according to methods described in the literature.[18,24−27] (11-(Acryloyloxy)undecyl)trimethylammonium bromide (AUTMAB) and (11-(methacryloyloxy)undecyl)trimethylammonium bromide (MUTMAB) were prepared upon reaction of 11-bromoundecanol-1 with acryloyl chloride or methacryloyl chloride, respectively, followed by ammonium salt formation upon treatment of the ω-brominated long chain ester with trimethylamine. (2-(Methacryloyloxy)ethyl)dodecyltrimethylammonium bromide (MEDDAB) was prepared upon reaction of dimethylaminoethyl-methacrylate with 1-bromododecane at 50 °C. Styrene (>99%) was purchased from Acros and distilled before use in order to remove inhibitor and oligomer impurities. *N*-Isopropylacrylamide (Acros) was recrystallized from toluene and *n*-hexane (volume ratio 1:2). Milli-Q water was used for all experiments. Deuterium oxide (eurisotop, 99,9%) was used

as a solvent for samples subjected to neutron scattering experiments.

2.2. Methods. The single phase regions of micellar surfmer−NiPAAm−water solutions, styrene−surfmer−water, and styrene−surfmer−NiPAAm−water microemulsions were determined visually from their transparency at 20 °C. The composition was changed by adding small amounts of NiPAAm to the water−surfmer mixtures, or by titrating styrene into surfmer−NiPAAm−water solutions. All samples were thoroughly homogenized using a Vortex mixer and thermostatted in a water bath.

Polymerization was carried out in screw-capped glass tubes or quartz cuvettes using degassed Milli-Q water. ^{60}Co-gamma radiation was used for polymerization. The dose rate was 128.3 Gy/h, and the temperature was 20 °C.

SANS measurements were carried out with the KWS2 instrument at FRM II, JCNS Garching, Germany. The neutron wavelength was 4.5 Å with $\Delta\lambda/\lambda = 0.2$. Scattering intensities were measured over a scattering range from 0.0047 to 0.27 Å^{-1} using sample-to-detector distances of 2 and 8 m. Samples were put in quartz cells of 1 mm path length and tightly closed with Teflon stoppers. Measurements were carried out at 20 °C. D_2O was used instead of H_2O in order to enhance the contrast. Two-dimensional scattering data were corrected pixelwise in the standard way for detector sensitivity, empty cell scattering, and dark current prior to radial averaging. They were absolutely calibrated via a secondary Plexiglas calibration standard.

SANS Analysis. SANS analysis was carried out in order to determine the size, shape, polydispersity, and charge of the micelles and microemulsions. In general, the expression for the differential scattering cross section, $d\Sigma(q)/d\Omega = I(q)$, of a dispersion of N_p monodisperse particles is given by[28,29]

$$I(q) = An_pP(q)S(q) + B$$

where $n_p = N_p/V$ is the number density of the particles, $P(q)$ is the particle form factor depending on the size and shape of the particle, $S(q)$ is the structure factor for the correlation between particles, A is a constant which depends on the contrast condition, and B is a constant representing the incoherent scattering background.

Structure factors are calculated using a Hayter−Penfold-type approach including a screened Coulomb (Yukawa) potential. For calculation of the form factor, several particle geometries were tested. In our systems, the best results were achieved assuming spherical particles. Details of the fitting procedure are given in the literature.[16] Standard nonlinear least-squares fitting (Levenberg−Marquardt algorithm) was used to define the best parameter set for each sample. The data were analyzed with volume fraction, micelle radius, Gaussian distribution of micelle radius, and two Yukawa interaction parameters, $\gamma = z^2L_b$, a measure for interaction strength, and the Debye length $\zeta = (4\pi L_bN_AI)^{1/2}$, a measure for interaction length, as free fitting parameters. A q-independent background scattering due to incoherent scattering mainly caused by hydrogen atoms was also considered and optimized. Model functions were convoluted with a resolution function to correct for smearing due to finite apertures and wavelength distribution. From the particle volume, the aggregation number N_{Agg} of the surfmer and N_{Sty} of styrene were calculated using the known molecular volumes and taking into account the hydration of the headgroup. The charge number z of the particles can be calculated from the Yukawa parameter γ, which allows the dissociation of the surfmer z/N_{Agg} to be determined.

The degree of swelling S is given by $(W_S - W_D)/W_D$, where W_S and W_D are the weights of the swollen and dry gels, respectively. S was determined as a function of time at constant temperature, the temperature being in the range between 20 and 60 °C. For the swelling and deswelling measurements, hydrogels of a volume of ca. 1.5 cm^3 previously prepared in quartz cuvettes ($5 \times 1 \times 1$ cm^3) were taken from the cuvette and immersed in 200 mL of thermostatted Milli-Q water for different time periods. The water uptake (or release) was determined gravimetrically by weighing the hydrogel prior and subsequent to the water treatment.

The lower critical solution temperature (LCST) was determined UV spectroscopically by measuring the gel transmission at 500 nm as a function of temperature. Measurements were carried out using a Perkin-Elmer Lambda 14 UV/vis spectrometer equipped with a thermostatted sample holder. For the measurements, hydrogel samples were used, which were previously prepared in quartz cuvettes ($5 \times 1 \times 1$ cm^3).

Dose vs conversion curves of the individual monomers were determined either gravimetrically or upon spectroscopic measurements. For polymerization, 10% (w/w) aqueous solutions of the monomers were prepared, filled into screw-capped glass tubes, and exposed to different γ radiation doses at 20 °C. After irradiation, hydroquinone was added to each sample in order to inhibit further polymerization. Poly-NiPAAm (P-NiPAAm) was precipitated from the aqueous solution by adding a 1:1 (v:v) mixture of water/methanol. The precipitate was collected and dried, and the weight was determined. Poly-MEDDAB (P-MEDDAB) is insoluble in water and directly precipitated upon gamma irradiation. The precipitate was collected and dried, and the weight was determined. Poly-AUTMAB (P-AUTMAB) and poly-MUTMAB (P-MUTMAB) are soluble in water, and therefore, the conversion to polymer was analyzed using ^{1}H NMR spectroscopy. The integral intensities of the vinyl CH signals between 5.85 and 6.40 ppm (AUTMAB) and 5.60 and 6.05 ppm (MUTMAB) were divided by the integral intensities of the signals from the CH_2 group adjacent to the acryloyl or methacryloyl group, respectively. The CH_2 signals were chosen because they remain unchanged upon polymerization. Prior to polymerization, the ratio was 1:2, while during polymerization it gradually decreases to zero.

The structure of the hydrogels was studied using scanning electron microscopy (SEM). SEM was performed using the SEM-Zeiss Neon 40. Vacuum dried samples were fixed to the microscope holder using conductive silver, followed by coating with gold (EMITECH K950X).

3. Results and Discussion

3.1. Phase Behavior of Surfmer−NiPAAm−Water Systems. Since we were interested in the preparation of clear, transparent hydrogels, it was necessary to start from clear aqueous solutions of the monomeric compounds. Therefore, first, the phase behavior of the ternary and quaternary mixtures was investigated and the clear−turbid phase boundaries were determined. In Figure 1, partial phase diagrams of the surfmer−NiPAAm−water systems with AUTMAB, MUTMAB, or MEDDAB as surfmers are shown. If only NiPAAm and no surfmer is present in the aqueous phase, a clear solution is formed up to a NiPAAm content of 22% (w/w). The presence of surfmer increases the NiPAAm solubility in the order MEDDAB ≪ MUTMAB ≈ AUTMAB. For example, the NiPAAm solubility can be increased to 34% (w/w), if either 10% MEDDAB or 5% AUTMAB are added. The difference originates from the T-type and H-type structure of the surfmers

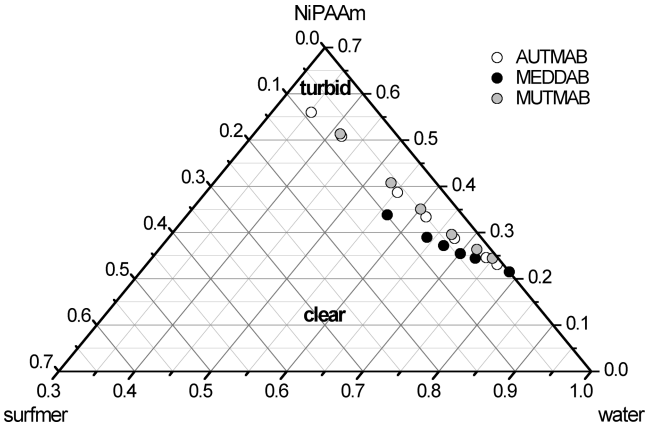

Figure 1. Partial phase diagram of the systems surfmer−NiPAAm−water indicating the clear/turbid boundary of the micellar solutions ($T = 20$ °C).

(the polymerizable group situated at the tail (T-) or head (H-) of the surfmer). In the H-type surfmer, the positive charge of the ammonium group is partially shielded by intramolecular interaction with the carbonyl group of the methacrylate unit,[26,30] whereas in the T-type surfmer any charge-transfer interaction is missing. As a result, the T-type surfmers are able to attract the polar, slightly amphiphilic NiPAAm molecules so that they become incorporated in the micellar shell (see also the neutron scattering results). The H-type surfmer is much less able to attract NiPAAm in the micellar shell, and therefore, the NiPAAm solubility in the system is lower.

3.2. Phase Behavior of Styrene−Surfmer−NiPAAm−Water Systems. The solubilization of hydrophobic compounds in the core of the micelles offers a possibility to modify the hydrogels. As an example, we studied the phase behavior of quaternary systems containing styrene as the fourth compound. In Figure 2, the phase diagrams of styrene−surfmer−NiPAAm−water systems with either MEDDAB, AUTMAB, or MUTMAB as surfmer are shown. In the diagrams, the ternary systems styrene−surfmer−water are also included, for comparison. It can be seen that the phase behavior of the MEDDAB-containing microemulsions is very different from the other systems. If no NiPAAm is present, the styrene solubilization of MEDDAB at 20 °C is lower (only 60%) than for AUTMAB, in good agreement with the results of a previous study.[16] The more hydrophobic character of MUTMAB causes the styrene solubilization of this surfmer to be higher. In a microemulsion containing 14% (w/w) AUTMAB, only 3.5% styrene can be solubilized, whereas in a system containing the same amount of MUTMAB up to 7% styrene can be included. All systems have in common that the solubility of styrene increases with the surfmer content.

If 10% (w/w) NiPAAm is present in the microemulsion, the styrene solubilization of the T-surfmers is lower, only about half of the value found for the system without NiPAAm. The reason is that NiPAAm is incorporated in the shell of the micelles (see the SANS studies below), which increases the curvature and decreases the size of the micelles. As a consequence, less styrene is incorporated. For microemulsions containing the H-monomer MEDDAB, the influence of NiPAAm is negligible up to a surfmer concentration of 5%. Surprisingly, at higher MEDDAB concentration, the styrene solubilization is strongly enhanced and becomes larger than in the NiPAAm-free system. For example, at a concentration of 15% (w/w) MEDDAB, up to 24% styrene can be solubilized, whereas in the corresponding NiPAAm-free system only 2.6% styrene is

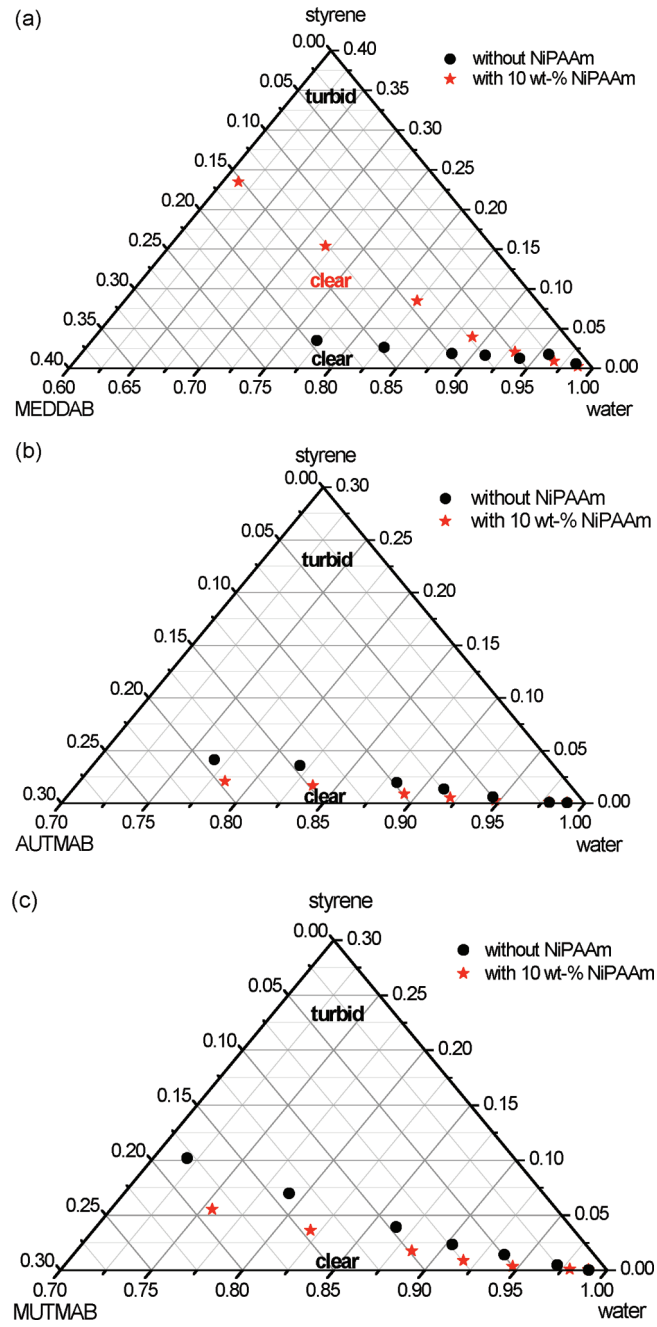

Figure 2. Partial phase diagrams of the systems styrene−surfmer−water and styrene−surfmer−NiPAAm−water indicating the clear/turbid boundary of the microemulsions ($T = 20$ °C).

soluble. The reason is not clear at present. We believe that the simultaneous presence of NIPAAm and styrene in higher concentration induces a structural transition into elongated micelles.

3.3. Structure Studies of Micellar and Microemulsion Systems. Structural studies were carried out using SANS measurements of monomeric micellar solutions containing NiPAAm and AUTMAB, MUTMAB, or MEDDAB. For comparison, micellar solutions of the surfmers without NiPAAm were also studied. Some microemulsion samples containing styrene were also investigated. Typical scattering curves from systems containing either AUTMAB, MUTMAB, or MEDDAB are plotted in Figure 3a, b, and c, respectively. The complete set of scattering data and fitted curves is shown in the Supporting Information. The data curves indicate the characteristic interaction peaks for dispersions of charged particles, which are due

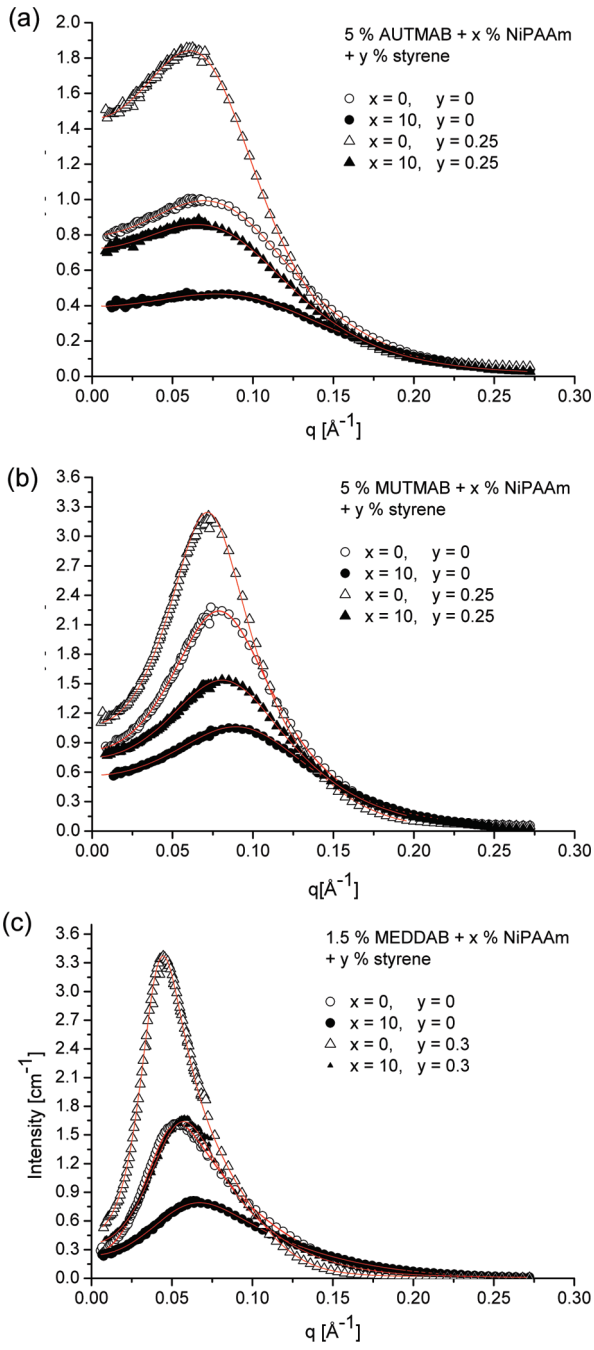

Figure 3. SANS spectra of surfmer micelles with and without addition of NiPAAm and/or styrene. The symbols represent the measured data points, and the solid lines are the model intensities.

to the corresponding peak in the interparticle structure factor $S_{(q)}$. The analysis of the scattering curves yielded appropriate fitting curves, which are also shown in Figure 3 as solid lines. In Table 1, the detailed fitting parameters (droplet volume fraction ϕ, micelle radius r_{mic}, Gaussian distribution of the micelle radius, and two Yukawa interaction parameters, γ and ξ) and the resulting droplet properties (volume of the micelles V, particle charge z, aggregation number N_{agg}, and fraction of dissociated surfactant z/N_{agg}) are compiled. Figure 3a shows SANS curves of the micellar AUTMAB solutions (concentration: 5% (w/w)) with and without addition of either styrene, NiPAAm, or both compounds. Data found for the pure micellar AUTMAB solution are in reasonable agreement with those reported in an earlier work.[16]

On addition of styrene, the maximum of the SANS curve is shifted to a lower q value and the intensity of the peak increases. This is consistent with a swelling of the micelles, the styrene being incorporated in the micellar cores leading to a globular o/w microemulsion. A comparable result was already reported[16] for the styrene−AUTMAB−water system containing 15% (w/w) AUTMAB and different amounts of styrene.

If NiPAAm is present instead of styrene, the maximum of the SANS curve is shifted to a higher q value. This indicates a smaller size of the micelles, which is consistent with an incorporation of the water-soluble but slightly amphiphilic NiPAAm in the shell of the micelles. The incorporation increases the curvature and decreases the size of the micelles. A corresponding picture illustrating either styrene or NiPAAm incorporation is shown in Scheme 3.

If NiPAAm and styrene are added, the q value is only little changed with regard to the pure micellar solution. Both effects—increase of the curvature of the shell and decrease of the curvature due to swelling of the core—compensate each other and cause only small amounts of styrene to be solubilized. This was already observed when the phase behavior was studied. The fitting parameters are compiled in Table 1. The scattering data are most accurately described by assuming a spherical shape of the micelles. For micelles of pure AUTMAB, the radius is 1.47 nm, for AUTMAB micelles in the presence of 0.25% (w/w) styrene, it is 1.85 nm, and in the presence of 10% (w/w) NiPAAm, it is 1.08 nm. In the presence of styrene and NiPAAm, the radius is 1.50 nm. Simultaneously, the aggregation number increases upon styrene addition and decreases upon NiPAAm addition. The dissociation of the surfmer headgroups remains constant upon the addition of styrene, because styrene is incorporated in the core and does not influence the polarity of the shell. However, the dissociation increases if NiPAAm is added. The reason is that neutral NiPAAm molecules are incorporated in the shell, and the micelles can only remain stable, if more surfmer headgroups dissociate.

SANS curves of micellar MUTMAB solutions (concentration: 5% (w/w)) are shown in Figure 3b. The changes observed on addition of styrene and NiPAAm are comparable with AUTMAB, the other T-surfmer, indicating that styrene is again solubilized in the micellar core and NiPAAm in the hydrophilic shell. The radius of the MUTMAB micelles is 1.78 nm, i.e., slightly larger than that for AUTMAB due to a higher aggregation number and the presence of the larger methacrylate unit. Upon addition of 0.25% styrene, the radius increases to 2.05 nm, and upon addition of 10% (w/w) NiPAAm, it is decreased to 1.44 nm. In the presence of both compounds, the micellar radius is comparable with the pure MUTMAB micelles, the general behavior being very similar to AUTMAB.

SANS curves of micellar MEDDAB solutions are shown in Figure 3c. The SANS curve of the micellar solution and the corresponding fit parameters are in good agreement with those reported previously.[16] However, in disagreement with the previous results, it was possible to fit the scattering curve by assuming a perfectly spherical shape of the micelles. Changes of the scattering curves observed upon addition of styrene and NiPAAm again are qualitatively similar to what has been observed for the other surfmers. However, the amount of solubilized styrene was much smaller due to the H-surfmer structure. In the presence of 0.3% (w/w) styrene, the radius increased from 2.01 to 2.76 nm, whereas in the presence of 10% (w/w) NiPAAm it decreased to 1.60 nm. If both additives were present, the original radius was nearly maintained. It is striking that the MEDDAB micelles exhibit a larger aggregation

TABLE 1: Parameters from SANS

surfmer	surfmer [% (w/w)]	styrene [% (w/w)]	NiPAAm [% (w/w)]	ϕ [%]	r_{mic} [nm]	σ	ξ [Å]	γ [C^2 Å]	z [C]	V [nm^3]	N_{agg}	z/N_{agg} [C]
AUTMAB	5	0	0	2.47	1.47	0.37	11.75	43.10	2.46	13.25	20.54	0.12
	5	0	10	2.30	1.08	0.58	10.49	29.31	2.03	5.28	8.44	0.24
	5	0	15	2.95	0.95	0.95	10.53	23.53	1.82	3.63	5.90	0.31
	5	0.25	0	2.68	1.85	0.35	11.27	152.77	4.63	26.37	38.85	0.12
	5	0.25	10	2.19	1.50	0.34	9.70	96.27	3.68	14.02	20.94	0.18
MUTMAB	5	0	0	3.54	1.77	0.25	15.45	69.44	3.12	23.14	32.88	0.10
	5	0	10	3.08	1.44	0.31	11.63	68.31	3.10	12.42	18.00	0.17
	5	0	15	3.26	1.34	0.43	11.11	50.14	2.65	10.09	14.63	0.18
	5	0.25	0	3.57	2.05	0.19	14.37	204.35	5.36	36.20	49.23	0.11
	5	0.25	10	3.12	1.69	0.19	12.46	99.10	3.73	20.20	27.62	0.14
MEDDAB	1.5	0	0	1.36	2.01	0.17	44.40	25.26	1.88	34.13	44.81	0.04
	1.5	0	10	1.35	1.60	0.23	28.92	20.00	1.68	17.22	22.76	0.07
	1.5	0	15	1.40	1.56	0.24	22.75	19.27	1.65	15.75	20.84	0.08
	1.5	0.3	0	1.80	2.67	0.16	32.55	122.31	4.15	79.68	87.84	0.05
	1.5	0.3	10	1.95	2.08	0.27	30.85	30.85	2.36	37.46	41.37	0.06

number, and that the dissociation of the polar ammonium headgroups is much smaller. This might be caused by the low polarity of the headgroups originating from strong electrostatic interactions between the positively charged ammonium group and the carbonyl group of the methacrylate unit in the surfmer molecule as previously proposed.[24,28]

3.4. Polymerization. At first, the homopolymerization of NiPAAm and the two surfmers MEDDAB and AUTMAB was studied. Aqueous solutions containing 10% (w/w) of the monomers were exposed to different radiation doses. Then, the conversion to polymer was determined gravimetrically or upon ^{1}H NMR spectroscopy as described in the Experimental Section. As shown in Figure 4a, NiPAAm exhibits the fastest reaction. Doses of 4−7 kGy are sufficient to polymerize more than 90% of the monomer, in agreement with results from the literature.[31] The polymerization of AUTMAB is quite rapid, too. After irradiation with 15 kGy, a conversion to polymer of 90% is reached. MEDDAB and especially MUTMAB are less reactive, and short induction periods occur. For MUTMAB, about 70 kGy is needed to obtain about 85% conversion. In Figure 4b, dose vs conversion curves of aqueous solutions containing 10% (w/w) NiPAAm and 1.5% (w/w) surfmer are shown. The comonomer solutions show induction periods which are considerably larger than those for the individual compounds. Solutions containing the H-monomer MEDDAB were completely polymerized at a dose of 25 kGy, while those containing the T-monomers reached about 95% conversion at a higher radiation dose of 45−50 kGy. NiPAAm solutions containing MUTMAB were less reactive than AUTMAB-containing solutions. For solutions containing 10% (w/w) NiPAAm and a higher surfmer content of 5% (w/w), the length of the induction period was further increased and therefore an even higher radiation dose was necessary to reach a high conversion to polymer (see the Supporting Information). For the preparation of hydrogels, we therefore always exposed the comonomer solutions to high radiation doses of 80 kGy.

SCHEME 3: Assembly of NiPAAm in the Shell of the AUTMAB Micelles and Styrene in the Core of the Micelles

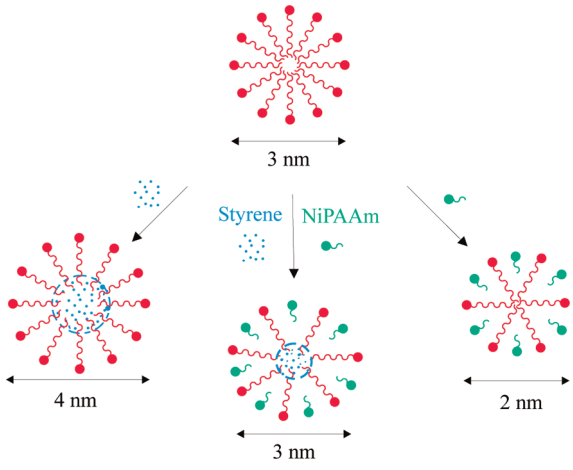

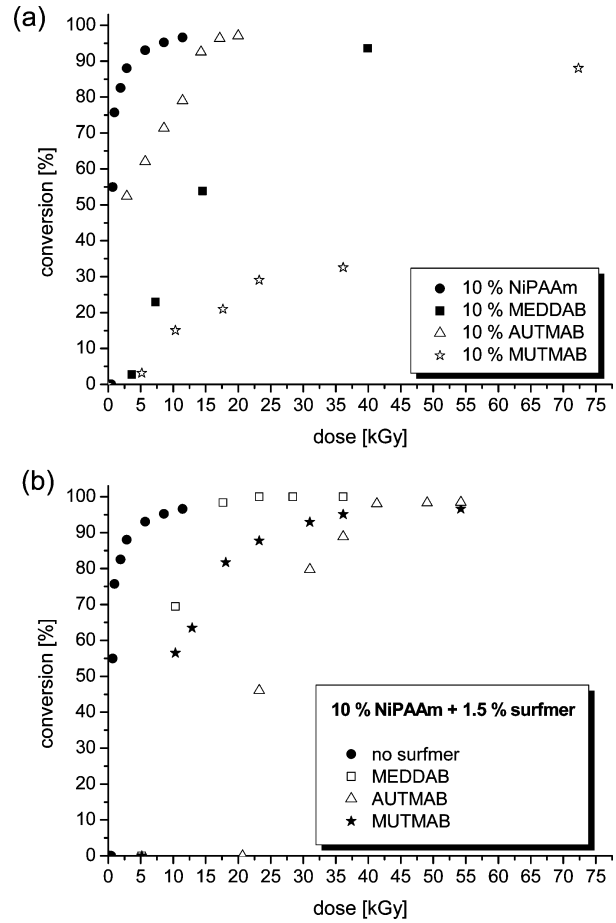

Figure 4. Dose vs conversion curves of pure surfmers and NiPAAm (a) and NiPAAm−surfmer comonomers (b) in aqueous solution (dose rate: 107.6 Gy/h, T = 20 °C).

TABLE 2: Composition of Aqueous Monomer Solutions and Transparency of Hydrogels

surfmer	surfmer [% (w/w)]	NiPAAm [% (w/w)]	styrene [% (w/w)]	transparency after 80 kGy
AUTMAB	10	10		clear
MUTMAB	5	10		clear
	7.5	10		turbid
MEDDAB	1.5	10		clear
	2	10		turbid
	1.5	10	0.3	clear
	2	10	0.4	turbid

Only clear comonomer solutions were used for polymerization, but some of the samples turned turbid during irradiation. The turbidity was dependent on the kind and amount of surfmer present in the system. The radiation-induced change in transparency was studied for a series of comonomer solutions containing 10% (w/w) NiPAAm and different amounts of surfmer (Table 2). While samples containing up to 10% AUTMAB remained clear upon irradiation, the samples containing 7.5% MUTMAB or 2% MEDDAB became turbid. The presence of an additional amount of 0.3% styrene in the MEDDAB-containing sample did not influence the behavior substantially. The change in transparency can be correlated with the hydrophilicity (and the water solubility) of the polymerized surfmers. While P-AUTMAB is readily water-soluble, P-MEDDAB is insoluble and precipitates from the aqueous phase. The solubility of P-MUTMAB is in between. Therefore, large amounts of MEDDAB or MUTMAB in aqueous NiPAAm solutions are not favorable for the preparation of transparent hydrogels.

The composition of the hydrogels was studied using IR spectroscopy. For this purpose, the gels were dried and subsequently analyzed. Attempts to leach out possible residual monomer or homopolymer were unsuccessful. Thus, it is very likely that only a cross-linked copolymer is formed. The C═O stretching modes at 1652, 1711, and 1652 cm^{-1}, respectively, indicate the presence of P-NiPAAm, P-AUTMAB, and P-MEDDAB in the gels (see the Supporting Information). Spectra of the corresponding homopolymers are also shown, for comparison. Additional information on whether statistical or block copolymers were formed could not be obtained from the spectra.

3.5. Structure of the Hydrogels. The structure of the hydrogels was studied using SEM. For this purpose, water was evaporated from the gels and the dry residue was investigated. Gels containing 10% (w/w) NiPAAm (and no surfmer) and NiPAAm and 1% (w/w) surfmer were investigated. SEM images of surfmer-containing hydrogels always show spherical aggregates of 30−50 nm in diameter distributed homogenously over the specimen, whereas pure NiPAAm gels exhibit a smooth structure (Figure 5). It is likely that the spherical aggregates originate from polymerized surfmer, which would support our structure model in Scheme 1. Compared to the monomer micelles, the polymerized aggregates are 5−10 times larger, indicating a growth during polymerization. The size increase may be due to surfmer transport to the polymerizing micelles, and to copolymerization with NiPAAm molecules in the shell of the micelles. In addition, aggregation of polymerized surfmer during drying of the gel may also contribute to the growth. Further structure studies using SANS and cryo-TEM will be carried out in the near future.

3.6. Lower Critical Solution Temperature. The LCST of the hydrogels was determined by measuring the changes in light transmittance at 500 nm as a function of temperature. The reference system was a pure NiPAAm hydrogel, which was obtained upon irradiation of a 10% (w/w) aqueous NiPAAm solution with a dose of 80 kGy. Influences on the LCST caused by different concentrations of surfmer and styrene and by a variation of the NiPAAm concentration were studied.

Let us begin with the pure NiPAAm-based hydrogel. As shown in Figure 6a, the gel has a very sharp transition from high to low transparency, if the LCST of the gel at 33.2 °C is reached. The transition is completely reversible. The presence of a small amount (0.5%) of AUTMAB increases the LCST to a value of 34.6 °C. For a higher AUTMAB concentration, the LCST is lower again until at a concentration of 5% (w/w) a value of 29.8 °C is reached. In the inset of Figure 6, the LCST is plotted versus the AUTMAB content. The LCST of the surfmer-containing hydrogels is controlled by two opposite effects. On one hand, the introduction of charged groups increases the hydrophilicity of the gel, and the LCST is raised. This effect dominates at low surfmer concentration. On the other hand, NiPAAm molecules are incorporated in the shell of the micelles, which influences the dissociation of the headgroups. As the SANS study has shown (see Table 1), the dissociation decreases, if at constant NiPAAm concentration, the surfmer content is increased. Therefore, at higher surfmer content, the hydrophilicity of the gel is lower and the LCST is lower as well.

In Figure 6b, the effect of an increase of the NiPAAm concentration is shown. The transmittances of gels with either 10 or 15% (w/w) NiPAAm and different amounts of AUTMAB are compared. For the pure NiPAAm gel, the influence is only weak. Since NiPAAm is less hydrophilic than water, an increase of the NiPAAm concentration from 10 to 15% (w/w) decreases the hydrophilicity of the gel and the LCST is lowered by 0.4 °C. Even smaller changes in the phase transition temperature are found if the NiPAAm content is increased in the presence of AUTMAB. The reason is that two opposite effects largely compensate each other. On one hand, the addition of NiPAAm decreases the hydrophilicity of the gel, but on the other hand, the NiPAAm molecules are partially incorporated in the shell of the micelles, where they increase the headgroup dissociation and thus the hydrophilicity. Therefore, the LCST of a gel containing 5% (w/w) AUTMAB is only little varied from 29.8 to 30.0 °C, if the NiPAAm content is increased from 10 to 15%.

In Figure 6c, the transmittance of NiPAAm hydrogels containing different amounts of MUTMAB, the other T-surfmer, is plotted versus the temperature. In general, the dependence of the LCST on the MUTMAB content follows the same trend

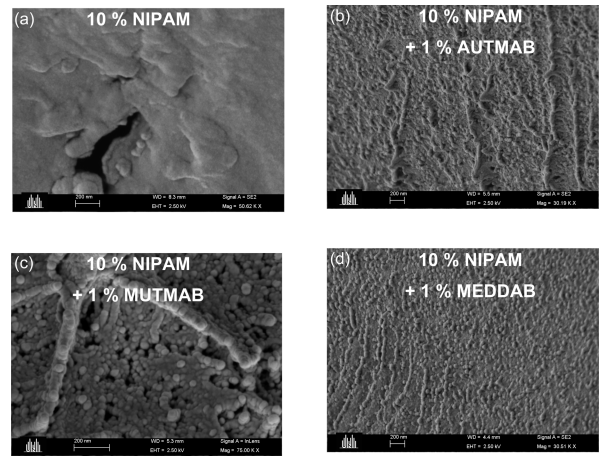

Figure 5. SEM images of poly-NiPAAm hydrogel (a) and copolymer hydrogels of NiPAAm−AUTMAB (b), NiPAAm−MUTMAB (c), and NiPAAm−MEDDAB (d).

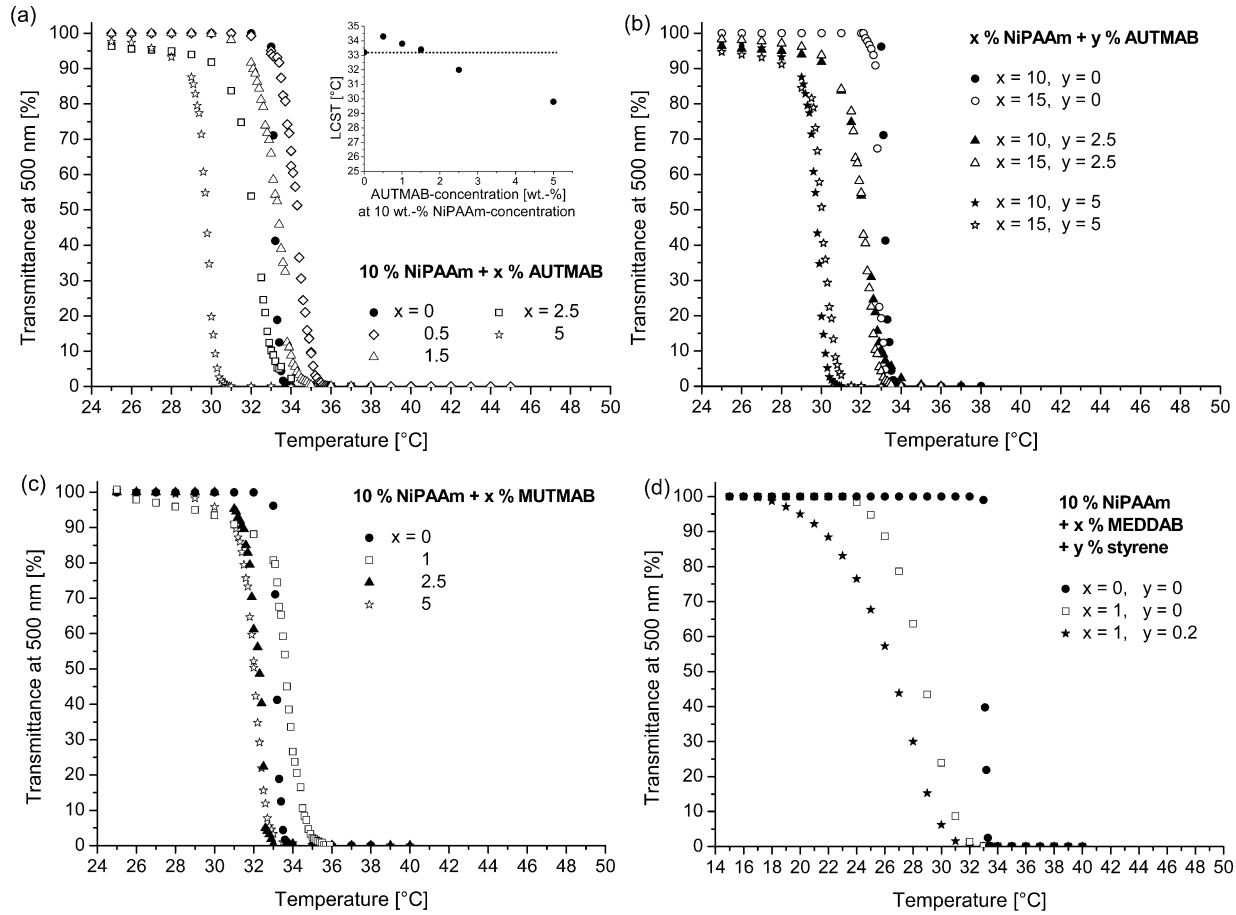

Figure 6. Transparency of various NiPAAm/surfmer hydrogels and pure P-NiPAAm gel as a function of temperature ($\lambda = 500$ nm).

as for AUTMAB. For a small MUTMAB content (1% (w/w)), the LCST is 0.5 °C higher than that for the pure NiPAAm gel. For 2.5 or 5% MUTMAB, the LCST is lower than that for the surfmer-free gel. The effect of MUTMAB on the LCST is generally smaller than that for AUTMAB. While 5% AUTMAB lowers the LCST to 29.6 °C, 5% MUTMAB only changes it to 32 °C. The reason is that the MUTMAB micelles are larger and for a certain surfmer concentration less micelles are present in the system. Consequently, the interaction with the aqueous phase is lower and the LCST is less affected.

In Figure 6d, the temperature dependence of the transmittance of NiPAAm hydrogels containing MEDDAB or MEDDAB and styrene is shown. Among all surfmers investigated, MEDDAB is the most hydrophobic, and the ion dissociation is lowest. Therefore, a gel containing only 1% (w/w) of the surfmer already exhibits a LCST of 28.5 °C. If styrene (concentration 0.2%) is present in addition, the hydrogel is even more hydrophobic and the LCST is only about 26.5 °C. Furthermore, the phase transition becomes rather broad, which can be ascribed to an inhomogeneous distribution of the polymerized styrene in the micelles. As a consequence, the phase transition sets in at different temperatures depending on the local polystyrene concentration in the gel.

3.6. Swelling Behavior. The swelling behavior was studied for hydrogels with different surfmer and NiPAAm content. Subsequent to irradiation with 80 kGy, the gels were immersed in pure water for different time periods and the weight increase (or loss) due to water penetration into (or out of) the samples was determined gravimetrically. The swelling ratio S was calculated as described in the Experimental Section.

In Figure 7a, swelling ratios at different temperatures are plotted versus the immersion time. It can be seen that the pure P-NiPAAm gel only exhibits a small increase in S at temperatures below the LCST. Above the LCST, the P-NiPAAm gel exhibits a moderate shrinking because water is expelled due to dehydration and collapse of the polymer chains. The swelling proceeds for several hours, whereas the shrinking is essentially finished after 1 h, although the original S value is not reached anymore. The reason is that dehydration starts at the sample surface and leads to skin formation, which renders diffusion of water from the interior of the gel increasingly difficult. As a consequence, the swelling is only poorly reversible (Figure 8a). In a swelling/shrinking cycle, the gel is first immersed in pure water at 20 °C for 8 h, and subsequently in water at 50 °C for another 8 h.

A different swelling/shrinking behavior is found if the hydrogels contain copolymerized surfmer compounds. As shown in Figure 7b for a gel based on 10% (w/w) NiPAAm and 1% (w/w) AUTMAB, the shrinking at 50 °C (or 60 °C) and the swelling at 20 °C (or 30 °C) are more pronounced than for the surfmer-free gel. The shrinking is essentially complete after 1 h. Already after 30 min, the S value has decreased by 50%. Swelling even goes on after several hours. At 30 °C, the S value is doubled within 1 h. For a sample swollen at 30 °C for 8 h, the swelling ratio is increased by a factor of 6. The strong swelling mainly originates from a high osmotic pressure caused by the presence of the charged surfmer molecules in the gel. The effect is especially obvious at 40 °C. This temperature is above the LCST, but the actually expected shrinking of the gel is overcompensated by the osmotic pressure-induced swelling. The osmotic effect can be suppressed if the hydrogels are immersed in a physiological salt solution. In this case, one observes a shrinking at 40 °C (see the Supporting Information). As shown in Figure 8b, the AUTMAB-containing hydrogel

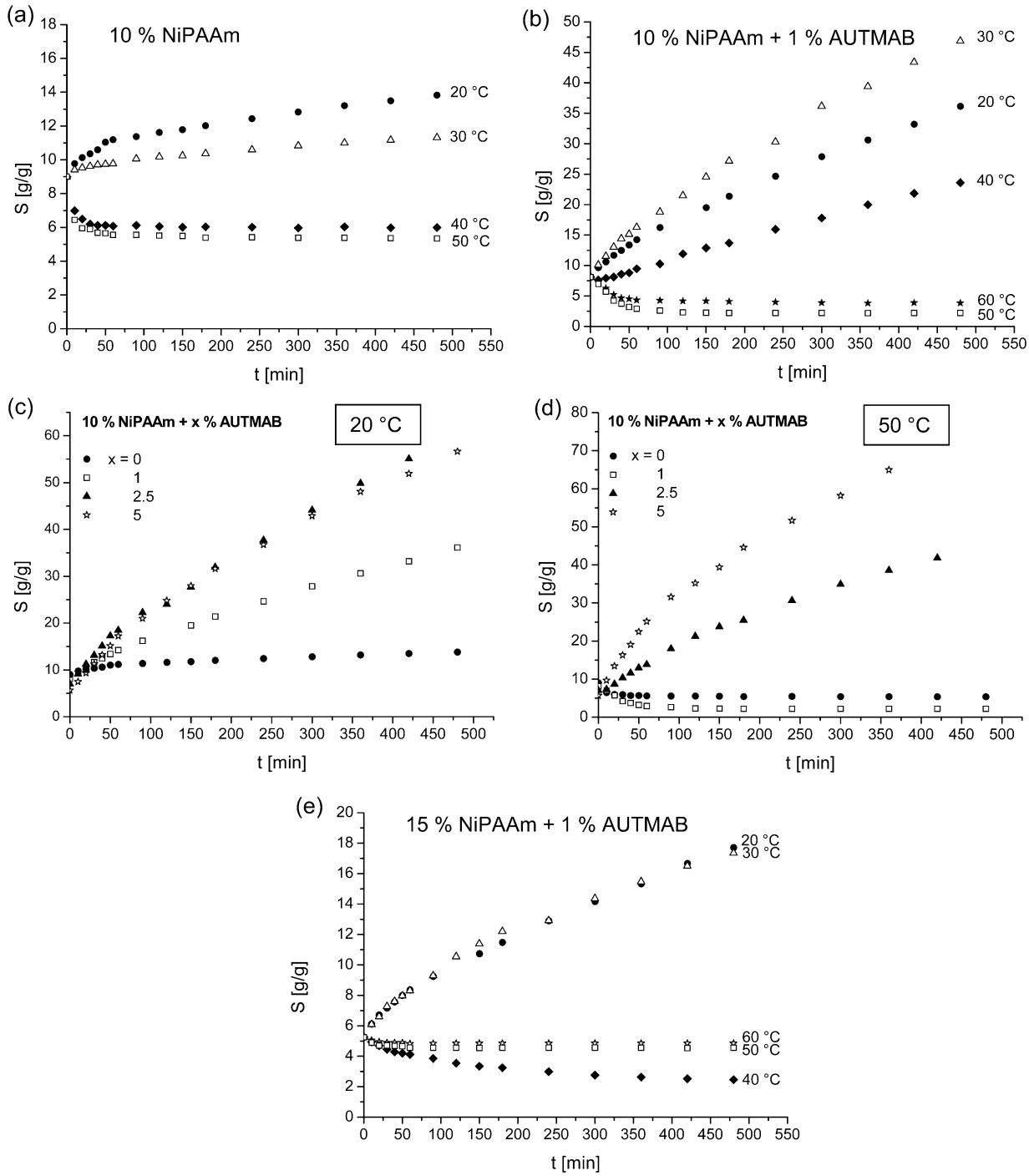

Figure 7. Swelling ratio *S* of pure P-NiPAAm (a) and AUTMAB/NiPAAm copolymer hydrogels of different composition (b−e) in water at different temperatures as a function of time.

exhibits an excellent reversibility in the swelling/deswelling behavior. Two reasons may be responsible for this: First, the gel is more stable than the pure NiPAAm gel, and second, the formation of an impermeable skin is prevented by the presence of the copolymerized micelles. The hydrophilic shell of the micelles renders the gels more permeable to water so that the original *S* value is completely recovered after a swelling/deswelling cycle at 20 and 50 °C, respectively.

We also studied the influence of a variation of the AUTMAB and NiPAAm content on the swelling behavior of the gel. Let us first concentrate on the increase of the AUTMAB concentration. In Figure 7c and d, swelling studies of samples containing 10% (w/w) NiPAAm and either no, 1, 2.5, or 5% AUTMAB are compiled. Studies were carried out at 20 and 50 °C, i.e., clearly below and above the LCST. The general trend is that the swelling increases with the surfmer content. With increasing surfmer content, the concentration of charged ammonium headgroups increases and a higher osmotic pressure builds up in the hydrogel. However, for the highest surfmer content of 5% and a temperature of 20 °C, the swelling is almost the same as for the sample with only 2.5% AUTMAB. The reason is that with increasing surfmer concentration the headgroup dissociation is lowered and thus the osmotic pressure is not further increased.

For samples studied at 50 °C, the headgroup dissociation is generally larger. Therefore, as shown in Figure 7d, the sample

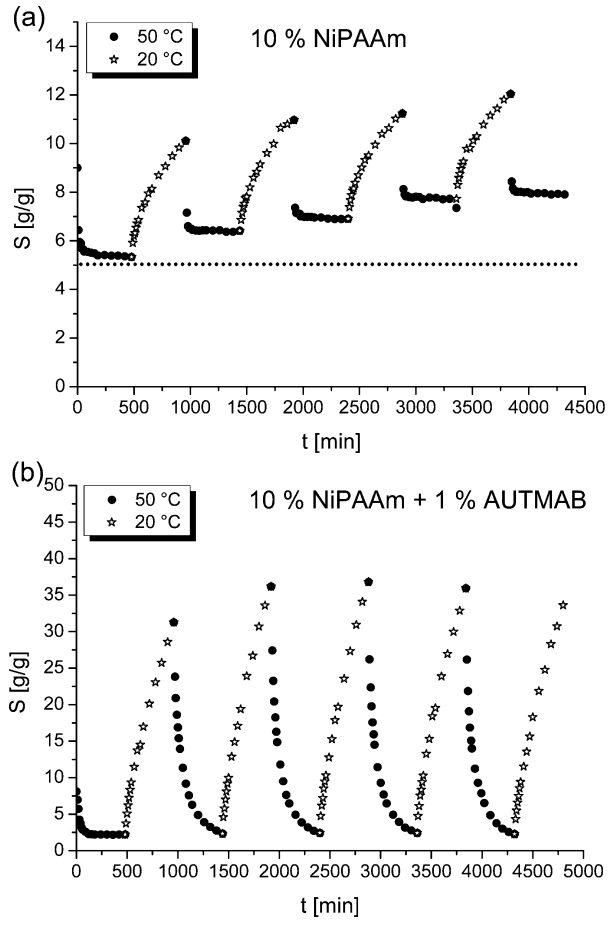

Figure 8. Reversibility of swelling of a pure NiPAAm hydrogel (a) and a hydrogel prepared from 1% (w/w) AUTMAB and 10% (w/w) NiPAAm in water (b). Samples were alternatingly immersed in water at 50 and 20 °C for 480 min in each case.

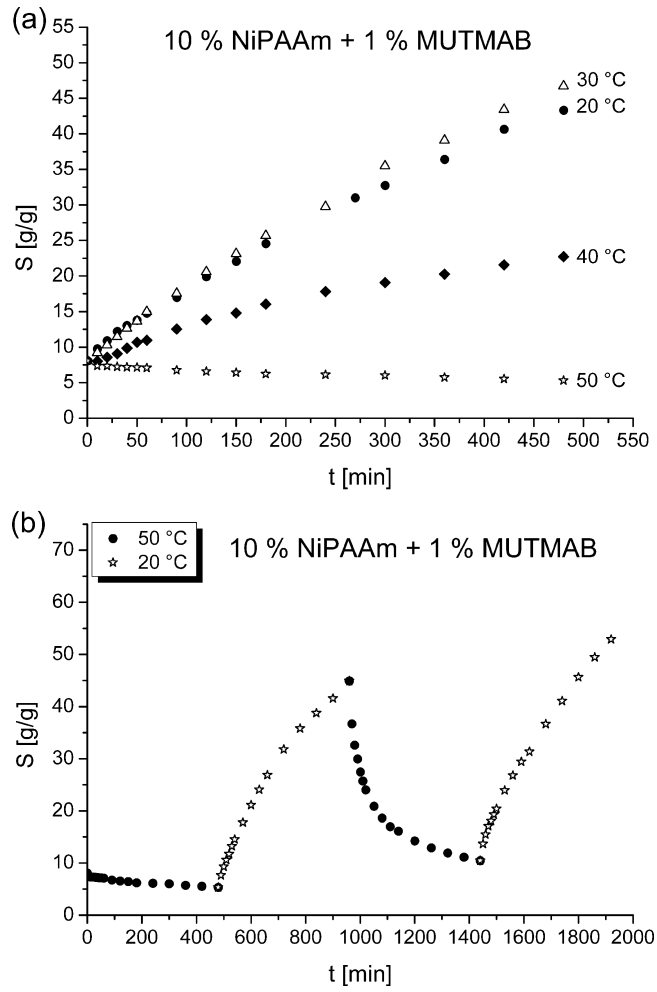

Figure 9. Swelling ratio of a hydrogel prepared from 1% (w/w) MUTMAB and 10% (w/w) NiPAAm in water at different temperatures as a function of time (a) and reversibility of the swelling (b). Samples were alternatingly immersed in water at 50 and 20 °C for 480 min in each case (b).

with the highest AUTMAB content of 5% (w/w) exhibits the highest swelling ratio. Within 6 h, the *S* value increases by a factor of 6.5. The reason is that above the LCST the polymer chains are dehydrated and aggregate. Due to the aggregation, pores are formed in the gel through which the water can easily permeate into the gel.

The NiPAAm content was also varied. Samples containing 1% AUTMAB and either 10 or 15% NiPAAm were studied (Figure 7b and e). In Figure 7e, it can be seen that swelling and shrinking are retarded if the NiPAAm concentration is increased. The lower swelling at 20 and 30 °C can be explained by a higher density of chemical cross-linking units in the gel. Due to the higher NiPAAm content, the network becomes less flexible and permeable so that the osmotic flow is retarded. At 40 °C, i.e., above the LCST, the highest shrinking is observed. At this temperature, the osmotic effect is overcompensated by the thermoresponsive behavior of the P-NiPAAm part of the gel. If the NiPAAm content was only 10%, the hydrogel was swelling at 40 °C (Figure 7b). If the temperature is higher than 40 °C, the shrinking is lower again. Due to the high P-NiPAAm content of 15% (w/w), a hydrophobic skin is formed at the surface (as in pure NiPAAm gels) retarding water diffusion despite the presence of the surfmer.

The temperature dependence of the swelling of MUTMAB−NiPAAm hydrogels is similar to the AUTMAB-containing gels. However, the difference in swelling at 20 and 30 °C is lower and the shrinking at 50 °C is slower than those for the AUTMAB-containing gel (Figure 9a). Due to the slower shrinking, the reversibility in swelling/deswelling is only poor (Figure 9b).

The small differences in swelling at 20 and 30 °C are the result of two effects, which partially compensate each other. On the one hand, the polymer−solvent interactions in the P-NiPAAm part of the network decrease with increasing temperature and the network becomes more hydrophobic. On the other hand, the dissociation of the surfmer headgroups increases with temperature and the network becomes more hydrophilic. For AUTMAB, the influence of the headgroup dissociation is clearly more pronounced, whereas for MUTMAB the headgroup dissociation is weaker and its influence dominates only slightly. For MEDDAB, it is shown below that both effects compensate each other completely and the swelling at 20 and 30 °C is identical. The high swelling ratios at 20 °C as well as the slow shrinking of MUTMAB hydrogels cannot be explained at present but may have deeper origin in the larger size of the micelles and a lower cross-linking density of the MUTMAB hydrogels compared with the AUTMAB gels. Studies of the mechanical properties supporting this assumption will be published shortly.[22]

In principle, the swelling behavior of MEDDAB−NiPAAm hydrogels follows the same trend as that observed for the AUTMAB- and MUTMAB-containing gels. However, MEDDAB

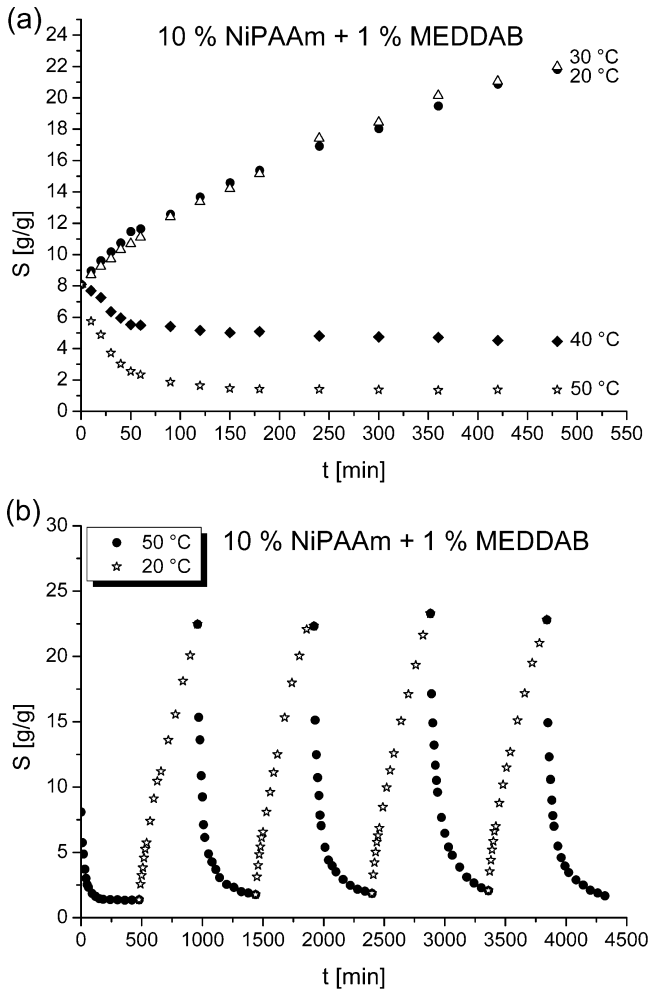

Figure 10. Swelling ratio of a hydrogel prepared from 1% (w/w) MEDDAB and 10% (w/w) NiPAAm in water at different temperatures as a function of time (a) and reversibility of the swelling (b). Samples were alternatingly immersed in water at 50 and 20 °C for 480 min in each case (b).

is more hydrophobic. Therefore, the shrinking above the LCST is more pronounced, and the swelling below the LCST is less intense (Figure 10a). For a gel containing 10% NiPAAm and 1% MEDDAB kept in water at 30 °C for 8 h, the increase in *S* is only half as large as that for a gel containing AUTMAB. Swelling and deswelling are well reversible (Figure 10b).

4. Conclusions

Different from previous work on surfactant-containing hydrogels, our study for the first time describes a single-step preparation of stable, NiPAAm-based hydrogels containing positively charged, copolymerized surfmer. The preparation method is based on radiation-induced copolymerization of NiPAAm and surfmer in an aqueous micellar solution, or microemulsion with solubilized styrene. Transparent gels with a solid content up to 20% are easily obtained if the comonomer ratio and concentration are properly chosen. The reaction simultaneously proceeds as a radical polymerization of NiPAAm, chemical cross-linking of NiPAAm chains, and copolymerization of NiPAAm and surfmer in micellar aggregates, resulting in a chemically and physically cross-linked, shape-persistent stable network structure. While the pure P-NiPAAm gel is easily disrupted under low compression, the gels polymerized from micellar solution or microemulsion can be reversibly compressed.[17] A quantitative study of the mechanical properties is at hand and will be published elsewhere.[22]

All surfmers reported in this study were suitable for copolymerization with NiPAAm and preparation of transparent hydrogels. Using the T-surfmers AUTMAB and MUTMAB, clear hydrogels could be obtained up to a concentration of 5% (w/w), whereas the more hydrophobic H-surfmer MEDDAB formed clear gels only, if the surfmer content was lower than 2%. SANS measurements of monomer solutions indicated the presence of spherical micelles. If styrene was solubilized in the micelles (and no NiPAAm was present in the system), the size of the micelles increased as expected. If NiPAAm (and no styrene) was present in the system, the micelles became smaller because NiPAAm was incorporated in the shell. If both compounds were present, the two effects compensated each other, and only small amounts of styrene could be solubilized.

At low concentration of ionic surfmer, the hydrogels exhibit a higher LCST due to the presence of the hydrophilic, positively charged headgroups in the network. At higher surfmer concentration, the LCST is lowered because the headgroup dissociation is decreased and the hydrophobic contribution from the alkyl chains begins to dominate. In surfmer-containing NiPAAm gels, a strong swelling is observed, which after several hours leads to a weight increase of approximately 600%. Swelling not only occurs below the LCST but also above because the charged headgroups of the surfmers give rise to a strong osmotic pressure, which overcompensates the shrinking due to dehydration and collapse of the P-NiPAAm chains. The effect can be suppressed if swelling/shrinking is carried out in physiological salt solution or if the cationic surfmers are replaced by nonionic ones.[32]

Using the one-step preparation described in this article, it is also possible to prepare pH-responsive hydrogels. In this case, NiPAAm has to be replaced by acrylic acid in the micellar solution. A detailed study of pH-sensitive, surfmer-containing hydrogels is at hand and will be published elsewhere.[32]

The presence of a high concentration of positively charged ammonium headgroups combined with the possibility to control the transport of water into and out of the gel via its thermoresponsive behavior offer the possibility to exchange the bromide counterions of the surfmers against other, functional counterions. Recent studies have shown that bromide can be easily exchanged against 1-pyrenesulfonate or 2,2′-azinobis(3-ethylbenzothiazoline-6-sulfonate),[33] introducing either luminescent or redox active properties in the hydrogel. Detailed studies on gel functionalization via counterion exchange will be published elsewhere.[23]

Acknowledgment. This research project has been supported by the European Commission under the seventh Framework Programme through the Key Action: Strengthening the European Research Area, Research Infrastructures. Contract No.: 226507 (NMI3). The DFG is thanked for financial support (project TI 219/10-1 and 10-2, priority program 1256 "Intelligent hydrogels"). Prof. Dr. K. Meerholz is thanked for providing the scanning electron microscope and Ruth Bruker for taking the SEM images.

Supporting Information Available: SANS scattering and fitting curves, table of fit parameters, IR spectra of hydrogels, polymerized surfmers, and P-NiPAAm, swelling ratio *S* vs time in water and salt solution, and dose vs conversion curve. This material is available free of charge via the Internet at http://pubs.acs.org.

References and Notes

(1) Schild, H. G. *Prog. Polym. Sci.* **1992**, *17*, 163.
(2) Hirokawa, Y.; Tanaka, T. *J. Chem. Phys.* **1986**, *81*, 6379.
(3) Dhara, D.; Chatterji, P. R. *Polymer* **2000**, *41*, 6133.
(4) Xulu, P. M.; Filipcsei, G.; Zrinyi, M. *Macromolecules* **2000**, *33*, 1716.
(5) Suzuki, A.; Tanaka, T. *Nature* **1990**, *346*, 345.
(6) Otake, K.; Inomata, H.; Konno, M.; Saito, S. *Macromolecules* **1990**, *23*, 283.
(7) Inomata, H.; Goto, S.; Otake, K.; Saito, S. *Langmuir* **1992**, *8*, 687.
(8) Heskins, M.; Guillet, J. E. *J. Macromol. Sci., Chem.* **1968**, *A2*, 1441.
(9) (a) Kuckling, D. *Colloid Polym. Sci.* **2009**, *287*, 881. (b) Tokarev, I.; Mtornov, M.; Minko, S. *J. Mater. Chem.* **2009**, *19*, 6932. (c) Schexnailder, P.; Schmidt, G. *Colloid Polym. Sci.* **2009**, *287*, 1.
(10) Yu, H.; Grainger, W. *Macromulecules* **1994**, *27*, 4554.
(11) Yan, H.; Fujiwara, H.; Sasaki, H.; Tsujii, K. *Angew. Chem., Int. Ed. Engl.* **2005**, *117*, 1987.
(12) Chen, X.; Tsujii, K. *Macromolecules* **2006**, *39*, 8550.
(13) Xu, X.-D.; Zhang, X.-Z.; Yang, J.; Cheng, S.-X.; Zhuo, R.-X.; Huang, Y.-Q. *Langmuir* **2007**, *23*, 4231.
(14) (a) Huang, T.; Xu, H.; Jiao, K.; Zhu, L.; Brow, H. R.; Wang, H. *Adv. Mater.* **2007**, *19*, 1622. (b) Haraguchi, H.; Li, H.-J. *Angew. Chem.* **2005**, *117*, 6658.
(15) Ming, W.; Zhao, Y.; Cui, J.; Fu, S.; Jones, F. N. *Macromolecules* **1999**, *32*, 528.
(16) Dreja, M.; Pyckhout-Hintzen, W.; Tieke, B. *Macromolecules* **1998**, *31*, 272.
(17) Friedrich, T.; Tieke, B. *Macromol. Symp.* **2010**, *287*, 16.
(18) Pawlowski, D.; Haibel, A.; Tieke, B. *Ber. Bunsen-Ges. Phys. Chem.* **1998**, *102*, 1865.
(19) Pawlowski, D.; Tieke, B. *Prog. Colloid Polym. Sci.* **2001**, *117*, 182.
(20) Pawlowski, D.; Tieke, B. *Langmuir* **2003**, *19*, 6498.
(21) Pawlowski, D.; Tieke, B. *Prog. Colloid Polym. Sci.* **2004**, *129*, 24.
(22) Stadler, F.; Bailly, C.; Friedrich, T.; Tieke, B. To be published.
(23) Friedrich, T.; Tieke, B. To be published.
(24) Nagai, K.; Obishi, Y *J. Polym. Sci., Part A: Polym. Chem.* **1994**, *32*, 445.
(25) Nagai, K.; Obishi, Y; Inaba, H.; Kudo, S. *J. Polym. Sci., Polym. Chem. Ed.* **1985**, *23*, 1221.
(26) Hamid, S. M.; Sherrington, D. C. *Polymer* **1987**, *28*, 325.
(27) Paleos, C.; Mangomenon-Leonidopoulou, G.; Malliaris, A. *Mol. Cryst. Liq. Cryst.* **1988**, *161*, 385.
(28) Hayter, J. B.; Penfold, J. *Colloid Polym. Sci.* **1983**, *261*, 1022.
(29) Chen, S.-H. *Annu. Rev. Phys. Chem.* **1986**, *37*, 351.
(30) McGrath, K. M.; Drummond, C. J. *Colloid Polym. Sci.* **1996**, *274*, 612.
(31) Maolin, Z.; Hongfei, H.; Jilan, W. *Radiat. Phys. Chem.* **1993**, *42*, 919.
(32) Friedrich, T.; Tieke, B. To be published.
(33) Song, H.-K.; Lee, E. J.; Oh, S. M. *Chem. Mater.* **2005**, *17*, 2231.

JP911358Z